Letters in Applied NanoBioScience
Open-Access Journal (ISSN: 2284-6808)

Review
Volume 15, Issue 2, 2026, 52
https://doi.org/10.33263/LIANBS152.052

In-silico and Literature-Based Perspectives of Astragalin as a Multi-Target Therapeutic Agent for Alzheimer's

Anish Singh [1], Diksha Dalal [2], Rajiv Sharma [1], Lovedeep Singh [1,*]

[1] University Institute of Pharma Sciences, Chandigarh University, Mohali, Punjab, India; anish.r262@cumail.in(A.S.); lovedeep.e13279@cumail.in (L.S.); principal.uips@cumail.in(R.S.);
[2] School of Pharmaceutical Sciences, CGC University, Mohali, Punjab, India;diksha.j4121@cgcuniversity.in;
* Correspondence: lovedeep.e13279@cumail.in;

Received: 4.08.2025; Accepted: 21.02.2026; Published: 30.06.2026

Abstract: Alzheimer's disease is a progressive neurodegenerative disorder characterized by the accumulation of Aβ plaques and tau protein neurofibrillary tangles, along with oxidative stress, chronic neuroinflammation, and progressive cognitive decline. A class of polyphenolic compounds, flavonoids, known for their anti-inflammatory and antioxidant properties, has shown promise in mitigating Alzheimer's disease pathology. Among them, the flavonoid glycoside astragalin (*kaempferol-3-O-glucoside*), found in plants such as *Astragalus membranaceus* and *Morus alba*, exhibits strong neuroprotective effects. It reduces neuroinflammation by inhibiting microglial activation and lowering pro-inflammatory cytokine levels, while its antioxidant activity protects neurons from Aβ-induced oxidative damage. Preclinical studies suggest that astragalin enhances mitochondrial function, reduces oxidative stress, and attenuates Aβ-induced neuroinflammation. The structure of astragalin was retrieved from the PubChem database and energy-minimized using Chem3D. The crystal structures of the target proteins were obtained from the protein data bank (PDB) and prepared by removing water molecules and adding polar hydrogens using AutoDock tools. Molecular docking was performed, employing a grid-based algorithm and standard scoring functions to predict binding affinities and key residue interactions. Visualization and 2D/3D interaction mapping were conducted using Discovery Studio Visualizer. Molecular docking studies further support its therapeutic potential: astragalin shows favorable binding affinity with Nrf-2, potentially activating antioxidant response elements; it interacts with Aβ (PDB ID: 1IYT) shows binding energy -30.8 kcal/mol, possibly stabilizing non-toxic conformations and preventing aggregation; and it binds within the ligand-binding domain of ERα (PDB ID: 1A52) shows binding energy -7.7 kcal/mol, suggesting a modulatory role in estrogen-mediated neuroprotection. It also interacts with Tau protein (Tau, PDB ID: 2mz7), which shows binding energy -29.9 kcal/mol, and NF-κB (PDB ID: 1NFK)shows binding energy -6.8 kcal/mol, suggesting a modulatory role in alzheimer's disease. These interactions, along with astragalin's ability to cross the blood-brain barrier and modulate key signaling pathways such as PI3K/AKT-mTOR, underscore its promise as a multi-targeted agent for future Alzheimer's disease therapies.

Keywords: Alzheimer's disease; molecular docking; astragalin; neurodegeneration.

1. Introduction

Alzheimer's disease (AD) is a neurodegenerative illness that results in amnestic cognitive impairment, whereas in its less common forms, it produces non-amnestic cognitive

impairment. The molecular characteristics of AD include tau-carrying neurofibrillary tangles and plaques containing Aβ [1]. After the age of 60, the incidence of AD doubles every five years, rising from 1% among those aged 60 to 64 to up to 40% among people aged 85 and above [2]. Aβ plaque buildup in the brain, oxidative stress, and neuroinflammation are all strongly linked to AD, which is characterized by gradual cognitive decline and neuronal death [3]. Nuclear factor kappa-light-chain-enhancer of activated B cells (NF-κB) was selected as a key regulator of neuroinflammation, a major contributor to disease progression, while estrogen receptor alpha (Erα) was chosen owing to its established neuroprotective, anti-inflammatory, and antioxidant functions reported in recent literature. Pathogenic mutations in presenilin may contribute to neurodegeneration independently of protein aggregation by impairing its essential trophic and cellular survival functions [4, 5]. The neuroprotective properties of flavonoids, a broad class of polyphenolic compounds found in a variety of fruits, vegetables, and beverages, have attracted interest, especially in relation to AD [6, 7]. Aβ plaques, neurofibrillary tangles, oxidative stress, and neuroinflammation are all strongly linked to AD, which is characterized by a gradual deterioration in cognitive function [8, 9]. By scavenging free radicals, flavonoids are known to control oxidative stress and lessen oxidative damage in neural cells [10-12]. Astragalin (*kaempferol-3-O-glucoside*), as shown in 3D and 2D structures in Figures 1 and 2, is a naturally occurring flavonoid glycoside present in several medicinal plants, including *Astragalus membranaceus* and *Morus alba*, which show anti-inflammatory, antioxidant, and anti-apoptotic properties that are especially important in neurodegenerative illnesses such as AD [13, 14]. Astragalin is a potential option for treating AD because of its capacity to alter these harmful processes. According to preclinical research, it may protect neurons from Aβ-induced damage by lowering pro-inflammatory cytokine levels and preventing microglial activation, thereby attenuating neuroinflammation [15]. Molecular docking studies support these findings by revealing astragalin's multi-target interactions with several key AD-related proteins. Docking with Aβ peptide (PDB ID: 1IYT) showed stable hydrogen bonding and hydrophobic interactions, suggesting inhibition of peptide aggregation. Interaction with ERα (PDB ID: 1A52) indicated potential modulation of neuroprotective estrogenic pathways. Interaction with Tau protein (Tau, PDB ID:2MZ7) shows that astragalin is a multi-target therapeutic agent for AD [16].

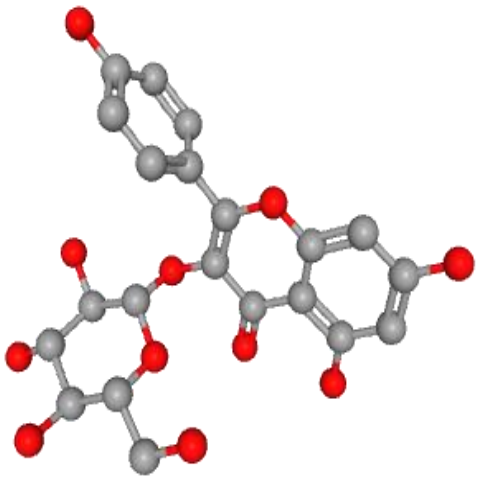

Figure 1. 3D structure of Astragalin.

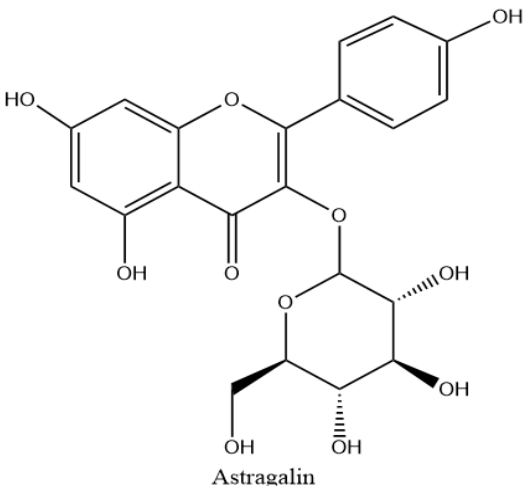

Astragalin

Figure 2. 2D structure of Astragalin.

Additionally, by strengthening cellular antioxidant defenses and scavenging free radicals, its antioxidant properties help reduce oxidative damage, a crucial factor in the

progression of AD [17]. Accumulating evidence suggests that astragalin may improve mitochondrial function and alleviate energy deficits associated with AD progression, further strengthening its potential as a therapeutic agent[18]. These complex effects indicate that astragalin is a promising candidate for further research into the development of treatments for AD [19]. Moreover, astragalin modulates oxidative stress-induced Aβ-mediated neuronal damage. In addition, it modulates the phosphoinositide 3-kinase (PI3K)/AKT-mammalian target of rapamycin (mTOR) signaling pathway to confer neuroprotection. Henceforth, drawing on existing literature elucidating astragalin's neuroprotective properties, the current review provides a detailed analysis of its mechanistic underpinnings in neuroprotection.

2. Pharmacokinetics Profile of Astragalin

Tao *et al.* reported that the time to reach maximum plasma concentration (Tmax) of astragalin in rats was 0.39 ± 0.14 hours, with an elimination half-life ($T_{1/2}$) of 0.31 ± 0.04 hours [20]. In comparison, He *et al.* found that the Tmax of astragalin in the total flavonoids from mulberry leaves was 0.19 ± 0.06 hours, while the $T_{1/2}$ extended to 0.87 ± 0.52 hours [21]. Xu *et al.* further observed that astragalin is rapidly absorbed from the rat gastrointestinal tract, appearing in plasma within 5 minutes, indicating a swift absorption and elimination profile [22]. In rats with myocardial ischemia-reperfusion injury (MIRI), pharmacokinetic parameters such as Tmax, Cmax, AUC_{0}-t, AUC_{0}-∞, MRT_{0}-t, and MRT_{0}-∞ were significantly elevated, while clearance (CL) was reduced, compared to normal rats [23]. Conversely, in renal insufficiency models, AUC_{0}-t, AUC_{0}-∞, and Cmax were lower, and both $T_{1/2}$ and Tmax were prolonged [23]. These findings suggest that pathological conditions can markedly influence the *in vivo* metabolism of astragalin. Moreover, Lu *et al.* reported that in MIRI rats, urinary and biliary excretion of astragalin decreased, while fecal excretion increased, suggesting that feces may become the predominant excretory route under such pathological conditions. Interestingly, the method of processing Cuscutae Semen also influenced astragalin absorption and bioavailability. Specifically, stir-fried Cuscutae Semen (SF-CS) resulted in a longer Tmax and reduced Cmax compared to salt-processed Cuscutae Semen (SP-CS) [24]. According to Liu, Zou *et al.*, salt-processing appears to enhance astragalin absorption and bioavailability by increasing its solubility in rats [25]. The compound exhibits low absorption, with a Caco-2 permeability of -6.33 logPapp, an MDCK value of -5.54 cm/s, and is predicted to be non-bioavailable (20% and 50%) and non-absorbed in HIA. It is a P-gp inhibitor (0.577) and a non-substrate (0.44) with skin permeability of 1.73 log Kp. Distribution properties include BBB log PS -4.23, penetrable BBB (0.001), fraction unbound 0.9, PPB 82.18%, and VDss 1.01 log L/kg. Metabolism predictions show non-inhibitor and non-substrate status across CYP1A2, 2C19, 2C9, 2D6, 3A4, BCRP, and OATP1B1/1B3. Excretion values indicate clearance 11.65 log ml/min/kg, half-life <3 h (0.319), and OCT2 non-inhibitor (0.345).

2.1. Bio-synthesis of Astragalin.

Astragalin is biosynthesized in plants through the glycosylation of kaempferol, a flavonoid aglycone, by UDP-dependent glycosyltransferases such as AtUGT78D2. This enzymatic process attaches a glucose molecule to the 3-hydroxyl group of kaempferol, forming kaempferol-3-O-glucoside. In engineered microbial systems such as *E. coli*, metabolic pathways are optimized to enhance the production of both kaempferol and astragalin from precursors such as naringenin [26]. Enhancements include introducing efficient UDP-glucose

synthesis modules and optimizing fermentation conditions, as shown in Figure 3 [27]. These strategies have enabled high-yield biosynthesis of astragalin for pharmaceutical and nutraceutical applications [28].

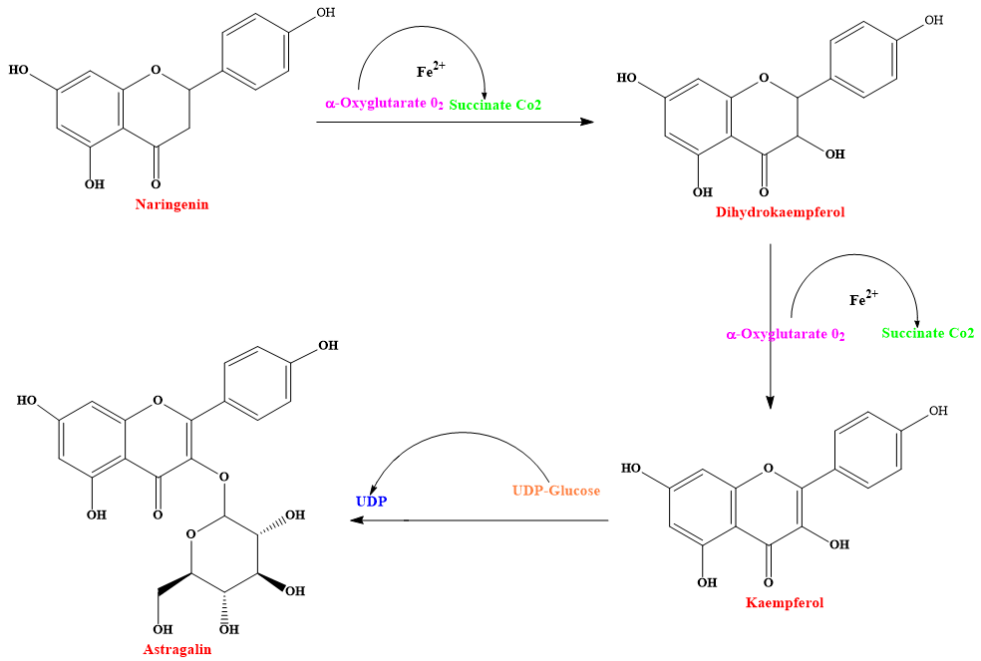

Figure 3. Biosynthesis of astragalin from precursors like naringenin

3. Molecular Docking

An *in silico* mode of designing drugs is a very good method that would require the design of drugs based on the predictability of ligand and receptor (disease target) interactions [29]. The PyRx software is used to perform the molecular docking analysis. Grid box dimensions are X × Y × Z Å, ensuring full coverage of the binding pocket. The most stable conformations of the compounds were carefully chosen and analyzed using the Discovery Studio 2025 Client software, version 20.1 [30].

3.1. Preparation of ligands.

The structure model has been created in a two-dimensional form, which has been achieved by the use of the MM2 functionality of Chem3D 16.0. The Mol2 file format is used to submit to the Swiss Dock server, and there is a button to prepare a ligand that you can use by clicking. The ligand structures were energy-minimized using the MMFF94 force field in Chem3D before docking, and their protonation states were assigned at physiological pH (7.4) using the open babel software.

3.2. Preparation of the receptor.

One can download the receptor/protein (PDB ID: 1iyt; 1a52; 1nfk; 2mz7) in the form of PDB by visiting the RCSB site (http://www.rscb.org). Removed the hetero atoms and water molecules of the receptor. The hydrogen was added together with the grid box. The clusters were further discussed in terms of binding energy, ligand efficiency, constant inhibitor, intermolecular energy, van der Waals interactions, electrostatic energies, etc. An interaction study was conducted on the ligand's binding mode and the most favorable binding-energy

conformation in PyMol and Discovery Studio Illumina. Molecular docking shows the binding of the ligands and the receptor, and the affinity of the ligands to the receptor.

3.3. Ligand-receptor binding interaction with 2D and 3D structures.

Ligand-receptor interactions in a molecular docking are computed to understand ligand-receptor binding to predict exactly how a small molecule (ligand) is fitted into the binding domain of a target protein (receptor). It consists of two main elements: the search algorithm to sample possible binding conformations, and the scoring function to approximate the binding strength using inter-atomic energies such as hydrogen bonding, van der Waals forces, and ruckelraumbeherts interactions [31].

3.4. 2D interaction diagrams.

Produced using the tools such as Discovery Biovia, graphically compact important contacts- the hydrogen bonds and hydrophobic contacts between ligand and receptor residues. The characteristics of some of the pharmacophoric features can be identified using these diagrams and further used in structure-activity relationship (SAR) studies [32].

3.5. 3D docking models.

Visual representations of the ligand, generated with tools such as PyMOL or AutoDock, provide a spatial view of the ligand within the receptor's binding cavity. Such models may be used to evaluate steric complementarity, conformational flexibility, and functional group orientation, thereby determining biological activity. These representations are complementary to one another in terms of comprehension and message conveyance, 2D and 3D, respectively, and thus act as invaluable tools in rational drug design and virtual screening [33].

3.6. Contact residue.

In molecular docking studies, contact residues are the specific amino acids within the receptor's binding site that directly interact with the ligand, forming the molecular interface critical for stabilizing the ligand-receptor complex. These interactions are typically non-covalent in nature, -such as hydrogen bonds, hydrophobic forces, π-π stacking, and electrostatic interactions, -and play a pivotal role in determining binding strength and specificity [34]. Amino acids like Asp, Glu, His, Tyr, Lys, and Ser frequently engage in these interactions due to their polar or charged side chains. Identifying these residues helps elucidate the binding mechanism and supports rational drug design by guiding the modification of ligand structures for improved affinity. Visualization tools such as PyMOL and Discovery Studio allow researchers to analyze these contacts in both 2D and 3D formats, offering valuable insights into receptor-ligand compatibility [35].

4. Validation of Docking

To ensure the accuracy and reliability of the docking protocol performed via the CB-Dock2 online server, we carried out re-docking of the native (co-crystallized) ligand for each selected receptor (PDB IDs: 1IYT, 1A52, 1NFK, and 2MZ7) using the same docking parameters. The docked poses were superimposed with the crystallographic conformations, and the root-mean-square deviation (RMSD) values were calculated. An RMSD of less than 2.0 Å

confirmed the validity and reproducibility of the docking protocol. Additionally, the validation results were cross-checked by analyzing the binding interactions and energy scores of the re-docked ligands using Discovery Studio 2025 and PyMOL, ensuring consistency with the original crystallographic binding orientations.

5. Docking Results

5.1. Docking of astragalin with Aβ protein having PDB ID: 1IYT.

Molecular docking of astragalin with the Aβ (1-42) peptide (PDB ID: 1IYT) reveals potential binding interactions that may inhibit amyloid aggregation. Astragalin, a flavonoid, likely forms hydrogen bonds with key residues in the helical regions of the peptide. This interaction could stabilize the peptide in a less toxic conformation, as shown in Table 1 and Figure 4. Such findings support astragalin's promise as a neuroprotective agent in Alzheimer's research.

Table 1. Various pocket IDs of amyloid beta and the binding score of astragalin

CurPocket ID	Binding score (Kcal)	Cavity volume (Å^3)	Center (x, y, z)	Docking size (x, y, z)
C4	-30.8 kcal/mol	13	0, -3, -8	22, 22, 22
C5	-29.8 kcal/mol	8	2, 1, -8	22, 22, 22
C2	-19.4 kcal/mol	17	-8, -5, 17	22, 22, 22
C3	-18.7 kcal/mol	15	-2, -3, 13	22, 22, 22
C1	-18.1kcal/mol	20	-6, 7, 17	22, 22, 22

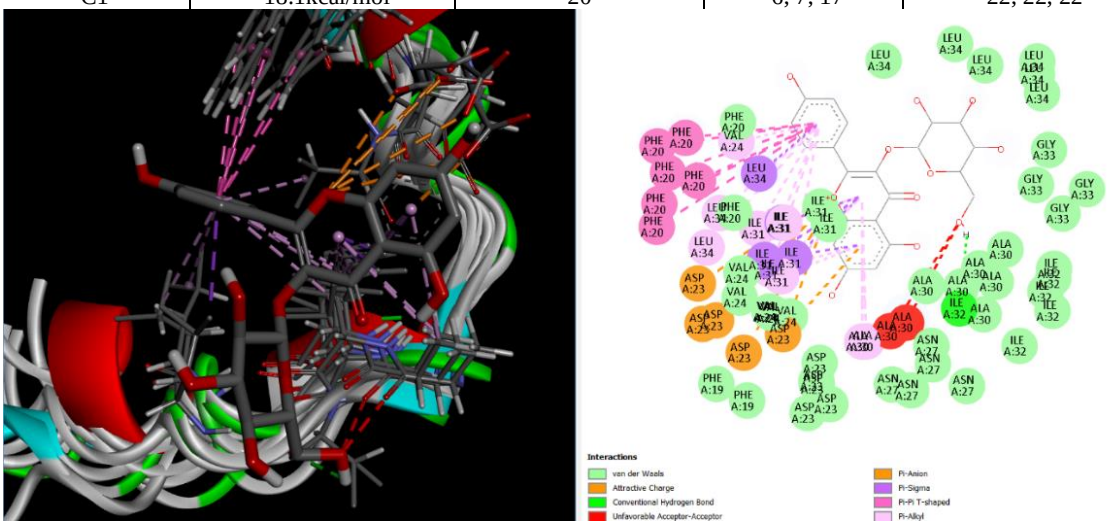

Figure 4. 3D and 2D docking interaction of ligand (astragalin) and receptor (Aβ).

5.2. Docking of astragalin with Tau protein having PDB ID: 2MZ7.

Molecular docking of astragalin with Tau protein (PDB ID: 2MZ7) suggests favorable binding interactions, particularly through hydrogen bonding and hydrophobic contacts within the microtubule-binding domain. These interactions may help stabilize Tau's conformation and potentially inhibit its pathological aggregation, offering a mechanistic basis for astragalin's anti-Alzheimer's potential as shown in Figure 5 and Table 2.

Table 2. Various pocket IDs of Tau protein and the binding score of astragalin.

CurPocket ID	Vina score	Cavity volume (Å^3)	Center (x, y, z)	Docking size (x, y, z)
C3	-29.9 kcal/mol	391	1, 5, -24	22, 22, 22
C2	-22.7 kcal/mol	529	18, -4, -10	22, 22, 22
C4	-12.9 kcal/mol	197	18, 12, -15	22, 22, 22
C1	-8.7 kcal/mol	1173	23, 9, -24	22, 22, 22
C5	-7.3 kcal/mol	167	-2, -19, -33	22, 22, 22

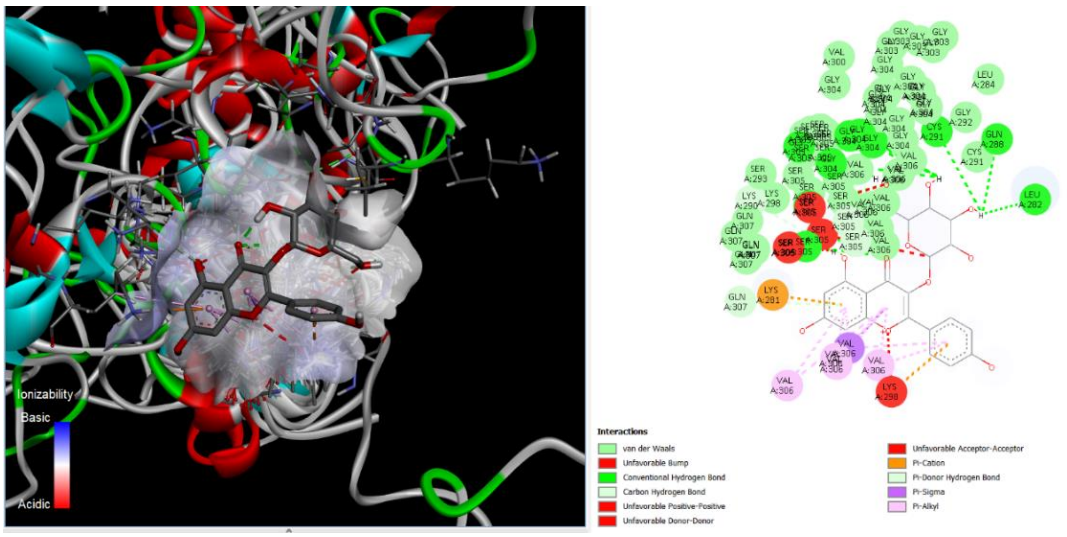

Figure 5. 3D and 2D docking interaction of astragalin with Tau protein (PDB ID: 2MZ7). The figure illustrates the molecular docking interaction of astragalin within the active site of the Tau protein. Hydrogen bonds, hydrophobic interactions, and π-π stacking are represented in the 2D view. The 3D model shows astragalin (in yellow) bound within the receptor cavity, surrounded by key interacting residues.

5.3. Docking of astragalin with NF-κB protein having PDB ID: 1NFK

Molecular docking of astragalin with the NF-κB p50 homodimer (PDB ID: 1NFK) suggests potential inhibitory interactions at the DNA-binding interface. Astragalin may form hydrogen bonds with key residues, potentially disrupting NF-κB's transcriptional activity, as shown in Table 3 and Figure 6. This interaction highlights its promise as an anti-inflammatory in AD.

Table 3. Various pocket IDs of nuclear factor kappa B and the binding score of astragalin

CurPocket ID	Binding score	Cavity volume (Å^3)	Center (x, y, z)	Docking size (x, y, z)
C3	-6.8 kcal/mol	1121	-19, -24, 30	22, 22, 22
C4	-6.4 kcal/mol	500	10, 13, 19	22, 22, 22
C5	-6.3 kcal/mol	307	28, 2, 19	22, 22, 22
C1	-6.2 kcal/mol	4929	-3, 18, 20	35, 35, 35
C2	-5.8 kcal/mol	2464	-1, 5, 20	22, 32, 22

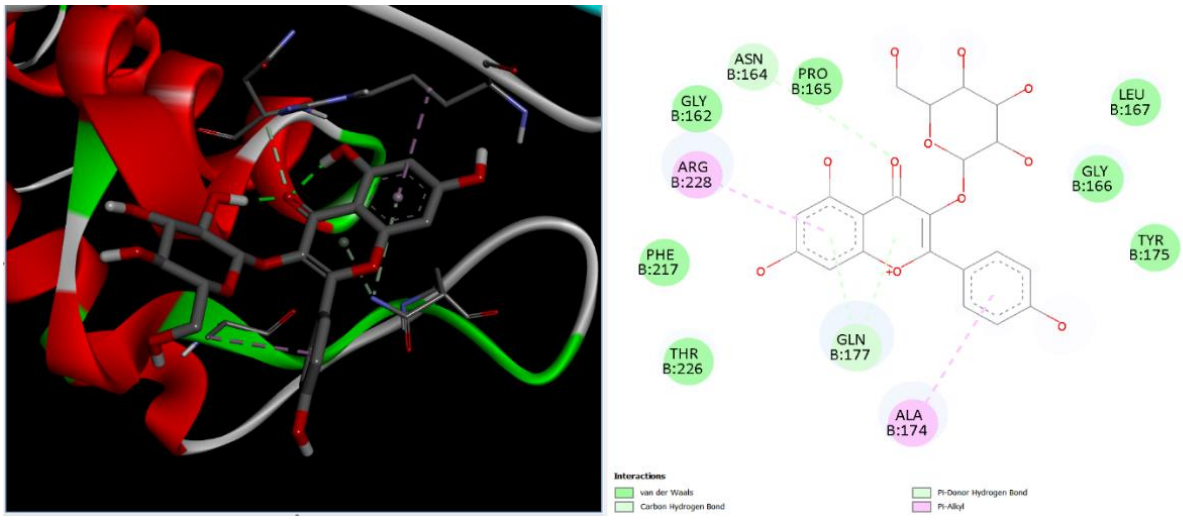

Figure 6. 3D and 2D docking interaction of astragalin with NF-κB (PDB ID: 1NFK). The 3D docking model demonstrates astragalin's binding orientation within the NF-κB active site, highlighting major hydrogen-bonded and hydrophobic interactions with catalytic residues. The 2D interaction diagram identifies specific amino acid contacts contributing to complex stabilization.

5.4. Docking of astragalin with ERα protein having PDB ID: 1A52.

Molecular docking of astragalin with ERα, (PDB ID: 1A52) suggests potential binding within the ligand-binding domain. Astragalin may interact via hydrogen bonding and hydrophobic contacts, possibly modulating receptor activity as shown in Table 4 and Figure 7. These interactions hint at its potential as a phytoestrogen or endocrine modulator.

Table 4. Various pocket IDs of Erα and the binding score of astragalin

CurPocket ID	Binding score	Cavity volume (Å^3)	Center (x, y, z)	Docking size (x, y, z)
C4	-7.7 kcal/mol	622	81, 24, 88	22, 22, 22
C2	-7.4 kcal/mol	2038	92, 16, 69	22, 32, 22
C3	-7.4 kcal/mol	781	113, 28, 84	22, 22, 22
C1	-6.9 kcal/mol	2084	104, 18, 100	22, 35, 22
C5	-6.4 kcal/mol	322	94, 14, 90	22, 22, 22

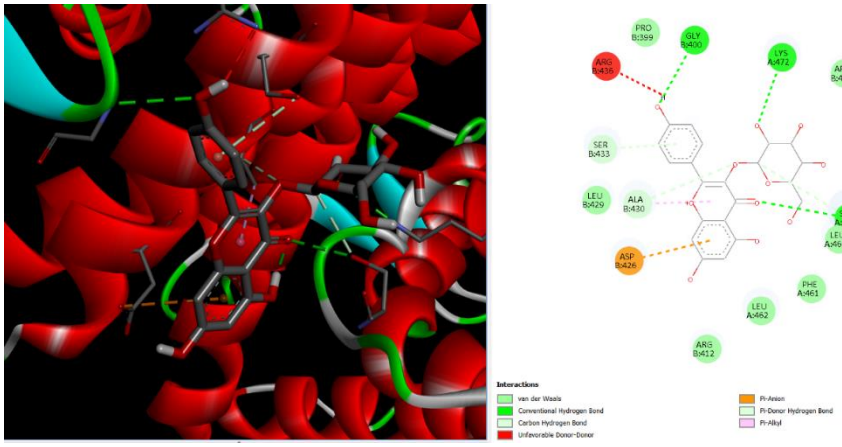

Figure 7. 3D and 2D docking interaction of astragalin with ERα (PDB ID: 1A52). This figure depicts the binding conformation of astragalin within the ligand-binding domain of ERα. The 3D view shows strong spatial complementarity between astragalin and the receptor pocket, while the 2D view details hydrogen bonds and hydrophobic contacts with key residues.

5.5. Comparative docking analysis of astragalin and donepezil.

Donepezil occupies the ligand-binding pocket with a highly stable conformation, supported by extensive hydrophobic interactions and key hydrogen bonds, resulting in a strong binding energy of -31.7 kcal/mol.

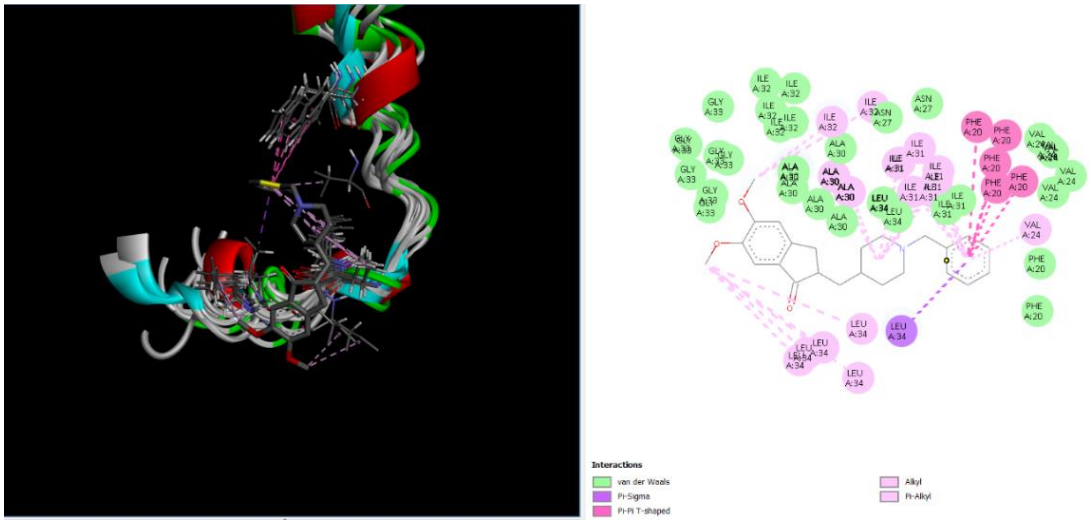

Figure 8. 3D and 2D docking interaction of donepezil with Aβ (PDB ID: 1IYT). This figure depicts the binding conformation of donepezil within the ligand-binding domain of Aβ.

In comparison, astragalin also aligns well within the same binding domain, showing good spatial complementarity and forming multiple stabilizing hydrogen bonds; however, its binding energy (-22.6 kcal/mol) indicates a relatively weaker, though still favorable, interaction with Aβ. The 2D interaction profiles further highlight that while donepezil achieves tighter binding through stronger hydrophobic contacts, astragalin relies more on polar interactions within the pocket. Despite the lower binding affinity, astragalin's interaction network suggests meaningful inhibitory potential, positioning it as a promising natural compound with complementary activity relative to the established standard inhibitor, as shown in Fig. 8.

6. Mechanistic insights of astragalin as an Anti-Alzheimer's agent

6.1. Astragalin modulates oxidative stress-induced Aβ-mediated neuronal damage.

Oxidative stress is a key player in the pathogenesis of AD. Increased oxidative stress reduced the levels of superoxide dismutase (SOD), catalase (CAT), and glutathione (GSH). Reduced antioxidant defense contributes to increased oxidative stress, thereby promoting the progression of AD. To date, several studies have revealed the astragalin effect in AD. Several lines of evidence suggest that increased oxidative stress elevates Aβ levels in the brain. Moreover, several researchers revealed that increased Aβ and oxidative stress cause neuronal damage [36]. Moreover, numerous studies have indicated that astragalin might confer neuroprotection by decreasing oxidative stress and Aβ [37, 38]. A report by Liu et al documented that astragalin (10 mg/kg) reduced the increased deposition level of Aβ1-40 and Aβ1-42. Moreover, it also decreased the beta-carboxyl-terminal fragment (β-CTF) level and tau-phosphorylation in SAMP8 mice. Furthermore, it also increased alpha-carboxyl-terminal fragment (α-CTF) protein and glycogen synthase kinase-3 beta (GSK-3β) phosphorylation in the hippocampus part of the brain (SAMP8 mice). It also decreased Aβ1-42 oligomers in the SAMP8 mice model. Moreover, astragalin treatment increased the ERα and estrogen receptor beta (Erβ) levels in the SAMP8 mice model [37]. Yang *et al.* documented that astragalin reduced cognitive dysfunction and decreased hippocampal neuronal damage. It also decreased the Aβ level in the hippocampus of amyloid precursor protein (APP)/presenilin 1 (PS1) mice. Astragalin activated the level of autophagic flux-related protein that results in autophagy in APP/PS1 mice [38]. SDA test revealed that astragalin (20, 40 mg/kg) upregulated the step-down latency, and the number of errors was lowered in APP/PS1 mice. The Morris water maze (MWM) test also showed that astragalin downregulated the escape latency time. Moreover, it also decreased the frequency of reaching the target platform. Furthermore, it enhanced the cognitive deficits of APP/PS1 mice. It decreased the score of neuronal damage grade in the hippocampus of mice. Additionally, astragalin (20, 40 mg/kg) improves the number of Nissl bodies in the hippocampus of the APP/PS1 mice brain. The HE and Nissl staining test revealed that astragalin downregulated the histopathological changes and neuronal loss in the hippocampus part of the brain. Furthermore, it reduced the hippocampal neuronal damage. Moreover, it decreased the Aβ accumulation in the brain. In addition to this, astragalin (40 mg/kg) decreased the SPs level. Astragalin (20, 40 mg/kg) reduces the Aβ and Aβ42 levels in serum, as shown in Table 5 [39].

Table 5. *In vitro* and *in vivo* studies of astragalin to confer neuroprotection

Sr. no	Model	Dose	Effect	Ref
1.	SAMP8 Mice Model	10 mg/Kg	• Reduced the increased deposition level of Aβ1-40 and Aβ1-42.	[37]

Sr. no	Model	Dose	Effect	Ref
			• Decreased β-CTF level. • Decreased tau phosphorylation. • Increased α-CTF level. • Increased GSK-3β phosphorylation. • Decreased Aβ1-42 oligomers. • Increased ERα and Erβ.	
2.	APP/SP1 Mice Model	20, 40 mg/Kg	• Decreased the Aβ and SP levels in the hippocampus. • Reduced the Aβ and Aβ42 levels in serum. • Reduced the expression of p-62. • Enhanced the ATG5, ATG12, and LAMP-1 expression. • Reduced the Aβ25-35 level in HT22 cells. • Increase the expression of LC3BII, Beclin-1, and LAMP-1.	[39]
3.	APP/PS1 transgenic Mice Model	10 mg/kg	• Enhanced the cognitive disorder • Decreased the escape latency, average speed, platform crossing frequency, and time. • Decreased the escape latency and total travel distance of mice. • Reduced the IL-6, IL-β and TNF-α in brain tissue. • Reduced inflammatory responses.	[16]
4.	APP/PS1 Mice Model	20, 40mg/kg	• Reduced the IBA-1 positive cell number and IBA-1 expression. • Decreased the Aβ Plaques and Aβ and Aβ42 levels in the serum of APP/PS1 mice. • Increased the level of LC3B and Beclin-1. • Reduced the level of p62. • Increased the level of ATG5, ATG12, and LAMP-I protein. • Decreased the expression of p-PI3K, p-Akt, and p-mTOR in the hippocampus of APP/PS1 mice.	[38]

By using autophagy in the APP/PS1 mice model, Yang *et al*. documented that astragalin enhanced the cognitive deficits of APP/PS1 mice.

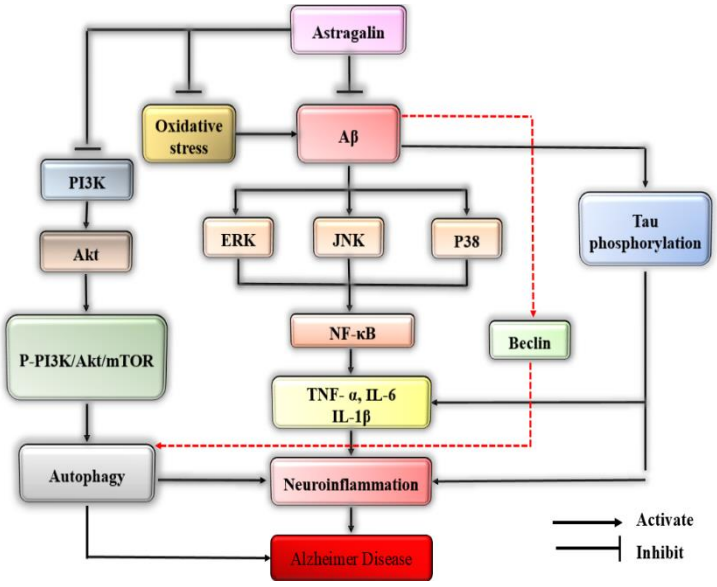

Figure 9. Role of astragalin in dephricizing AD along with various pathways. Astragalin mitigates AD progression by modulating multiple molecular targets. It reduces oxidative stress and inhibits Aβ accumulation, which subsequently downregulates c-Jun N-terminal kinase **(**JNK), extracellular signal-regulated kinase **(**ERK), and P38 signaling pathways. Astragalin suppresses NF-κB activation, leading to decreased pro-inflammatory cytokine production (TNF-α, IL-6, IL-1β) and reduced neuroinflammation. Concurrently, Astragalin activates the PI3K/Akt/mTOR pathway, enhancing autophagy and inhibiting Tau phosphorylation. The combined effects alleviate neuronal damage and attenuate AD progression.

Moreover, astragalin (20, 40 mg/kg) increased the latency and decreased the number of errors in APP/PS1 mice. Furthermore, astragalin at a dose of 40 mg/kg decreased the Aβ plaques in APP/PS1 mice. Literature review suggested that increased Aβ upregulated the pro-apoptotic protein level and apoptosis in the mouse body. Furthermore, due to increased apoptosis, the neuronal damage occurred [40]. Enzyme-linked immunosorbent assay (ELISA) revealed that APP/PS1 mice treated with astragalin (20, 40 mg/kg) for one month decreased the Aβ and Aβ1-42 levels in serum. APP/PS1 mice treated with astragalin (40 mg/kg) improved the level of LC3B and Beclin-1. Moreover, it also reduced the level of p62 to different degrees. Additionally, astragalin (40 mg/kg) increased the level of ATG5 and ATG12 in a dose-dependent manner as shown in Fig. 9 [38].

Cell Counting Kit-8 (CCK8) assay revealed that astragalin treatment also reduced the $A\beta_{25-35}$ level in HT22 cells. Furthermore, it also reduced the increased apoptosis of Aβ25-35-injured HT22 cells. It also increased the expressions of LC3BII, Beclin-1, and LAMP-1 and suppressed the expression of p62 in $A\beta_{25-35}$-damaged-treated HT22 cells [39]. A report by Du et al documented that astragalin enhanced the cognitive disorder in mice. Moreover, it also lowered the escape latency, average speed, platform crossing frequency, total travel distance, and time in a dose-dependent manner in APP/PS1 transgenic mice. It also decreased the escape latency and total travel distance of mice. Oxidative stress plays a key role in inflammation and neuronal damage. Increased oxidative stress may increase the level of pro-inflammatory cytokines. Whereas, increased pro-inflammatory cytokines also increased the inflammation in neurons [41]. ELISA analysis also revealed that it reduced the interleukin-6 (IL-6), interleukin-1 beta (IL-1β), and tumor necrosis factor alpha (TNF-α) in brain tissue. Moreover, HE staining revealed that it also reduced inflammatory responses. Immunohistochemistry (IHC) staining analysis revealed that astragalin reduced the IBA-1-positive cell number and IBA-1 expression, as shown in Figure 9 [16].

6.2. Modulation of PI3K/AKT-mTOR signaling pathway to confer neuroprotection.

One important regulator of autophagy is mTOR, which is influenced by a variety of signaling pathways, including those that sense the cell's energy state and initiate or inhibit protein synthesis [42]. The PI3K and kinase AKT pathway is triggered by neurotrophin and growth factor receptors and involves the kinase mTOR as a downstream target. It promotes cell growth, differentiation, and survival while suppressing apoptotic signals [43]. By using autophagy in the APP/PS1 mice model, Yang *et al.* documented that astragalin decreased the phosphorylation of the PI3K/Akt-mTOR pathway. Furthermore, it reduced the level of the Akt inhibitor MK2206 and the mTOR inhibitor rapamycin. It also increased the Akt inhibitor MK2206 and the mTOR inhibitor rapamycin, which reduced autophagy in cells [39]. Furthermore, it increased the ratio of LC3BII/LC3BI and the expression of Beclin-1, but it reduced the expression of p62. Astragalin (40 mg/kg) enhanced ATG5, ATG12, and LAMP-1 expression in a dose-dependent manner. It stimulated the formation of autophagosomes in neurons of APP/PS1 mice. It also reduced the increased p-P13K/Akt, p-Akt/Akt, and p-mTOR/mTOR $A\beta_{25-35}$ injured HT22 cells [39]. Furthermore, astragalin (10, 20, 40 mg/kg) increased the level of LAMP-I protein; astragalin (40 mg/kg) decreased the expression of p-PI3K, p-Akt, and p-mTOR in the hippocampus of APP/PS1 mice [38].

7. Limitations and future directions

The present study primarily relies on *in silico* molecular docking and literature-based mechanistic analyses to elucidate Astragalin's neuroprotective potential against AD. Although the computational results provide valuable insights into target interactions and possible signaling modulation, they are inherently limited by the static nature of docking simulations and the absence of experimental verification. Factors such as protein flexibility, ligand dynamics, solvation effects, and physiological metabolism were not fully addressed in the current framework, which may influence the actual binding behavior and biological efficacy of astragalin. Future research should aim to overcome these limitations through comprehensive *in vitro* and *in vivo* studies. Experimental validation using neuronal cell lines and transgenic Alzheimer's models will be essential to confirm astragalin's affinity, pharmacokinetics, and functional outcomes. We integrated our docking findings with targeted literature evidence linking each prioritized target to Alzheimer's pathophysiology (Aβ production/aggregation, tau phosphorylation, cholinergic dysfunction, oxidative stress, and neuroinflammation), thereby strengthening the biological plausibility of astragalin's multi-target activity while noting that experimental validation is required. Moreover, integrating molecular dynamics simulations, quantitative structure-activity relationship (QSAR) analyses, and omics-based approaches could further clarify its multi-target mechanisms and therapeutic relevance.

8. Conclusions

In conclusion, astragalin emerges as a promising multi-target therapeutic candidate for AD, addressing several interconnected pathological hallmarks, including oxidative stress, neuroinflammation, apoptosis, and Aβ aggregation. Its mechanistic action through modulation of the PI3K/AKT-mTOR pathway underscores its neuroprotective potential, validated further by the reversal of effects via autophagy inhibition. Molecular docking studies provide compelling evidence for astragalin's ability to interact with Aβ, Tau, and ERα, suggesting not only inhibitory effects on plaque formation but also potential neuroprotective enhancement via hormonal pathways. Moreover, the biosynthetic viability of astragalin through enzymatic glycosylation of kaempferol and scalable microbial production platforms adds significant value in terms of accessibility and future pharmaceutical development. Altogether, the mechanistic and structural insights from both experimental and *in silico* studies position astragalin as a plant-derived compound with powerful, multimodal efficacy in combating AD, warranting further translational and clinical exploration. However, it is important to emphasize that these findings are derived solely from computational simulations and literature-based analyses. Thus, the predicted interactions and mechanistic interpretations should be considered preliminary. The absence of experimental validation represents a limitation of this study. Future investigations should include *in vitro* and *in vivo* models to verify astragalin's binding efficacy, pharmacokinetic behavior, and neuroprotective mechanisms. Such studies would be essential to substantiate the current computational findings and to evaluate the therapeutic potential of astragalin as a multi-target agent for AD.

Author Contributions

Conceptualization, L.S. and A.S.; methodology, A.S.; software, R.S.; validation, R.S., L.S., and A.S.; formal analysis, D.D.; investigation, L.S.; resources, R.S.; data curation, A.S.; writing—original draft preparation, D.D.; writing—review and editing, L.S.; visualization,

R.S.; supervision, L.S. All authors have read and agreed to the published version of the manuscript.

Institutional Review Board Statement

Not applicable.

Informed Consent Statement

Not applicable.

Data Availability Statement

Not applicable.

Funding

No funding.

Acknowledgments

The authors are thankful to UIPS and Chandigarh University for their support and encouragement in this work.

Conflicts of Interest

There is no conflict of interest.

Abbreviations

The following abbreviations are used in this manuscript:

Abbreviation	Definition
AD	Alzheimer's Disease
Aβ	Amyloid Beta
ERα	Estrogen Receptor Alpha
TNF-α	Tumor Necrosis Factor Alpha
PDB	Protein Data Bank
ELISA	Enzyme-Linked Immunosorbent Assay
SAR	Structure-activity Relationship
NF-κB	Nuclear Factor Kappa B
CAT	Catalase
GSH	Gluthathione
SOD	Superoxide Dismutase
MWM	Morris Water Maize

References

1. Knopman, D.S.; Amieva, H.; Petersen, R.C.; Chételat, G.; Holtzman, D.M.; Hyman, B.T.; Nixon, R.A.; Jones, D.T. Alzheimer Disease. *Nat. Rev. Dis. Primers* **2021**, *7*, 33, https://doi.org/10.1038/s41572-021-00269-y.
2. Cummings, J.L.; Cole, G. Alzheimer's Disease. *JAMA* **2002**, *287*, 2335–2338, https://doi.org/10.1001/jama.287.18.2335.
3. Kása, P.; Rakonczay, Z.; Gulya, K. The Cholinergic System in Alzheimer's Disease. *Prog. Neurobiol*. **1997**, *52*, 511–535, https://doi.org/10.1016/S0301-0082(97)00028-2.

4. Xia, D.; Watanabe, H.; Wu, B.; Lee, S.H.; Li, Y.; Tsvetkov, A.; Bolshakov, V.Y.; Shen, J. Presenilin-1 Knockin Mice Reveal Loss-of-Function Mechanism for Familial Alzheimer's Disease. *Neuron* **2015**, *85*, 967–981, https://doi.org/10.1016/j.neuron.2015.01.021.
5. Mossello, E.; Ballini, E. Management of Patients with Alzheimer's Disease: Pharmacological Treatment and Quality of Life. *Ther. Adv. Chronic Dis.* **2012**, *3*, 183–193, https://doi.org/10.1177/2040622312452387.
6. García-Lafuente, A.; Guillamón, E.; Villares, A.; Rostagno, M.A.; Martínez, J.A. Flavonoids as Anti-Inflammatory Agents: Implications in Cancer and Cardiovascular Disease. *Inflamm. Res.* **2009**, *58*, 537–552, https://doi.org/10.1007/s00011-009-0037-3.
7. Spencer, J.P.E. Flavonoids and Brain Health: Multiple Effects Underpinned by Common Mechanisms. *Genes Nutr.* **2009**, *4*, 243–250, https://doi.org/10.1007/s12263-009-0136-3.
8. Selkoe, D.J. Alzheimer's Disease: Genes, Proteins, and Therapy. *Physiol. Rev.* **2001**, *81*, 741–766, https://doi.org/10.1152/physrev.2001.81.2.741.
9. Hardy, J.; Selkoe, D.J. The Amyloid Hypothesis of Alzheimer's Disease: Progress and Problems on the Road to Therapeutics. *Science* **2002**, *297*, 353–356, https://doi.org/10.1126/science.1072994.
10. Halliwell, B. Oxidative Stress and Neurodegeneration: Where Are We Now? *J. Neurochem.* **2006**, *97*, 1634–1658, https://doi.org/10.1111/j.1471-4159.2006.03907.x.
11. Pham-Huy, L.A.; He, H.; Pham-Huy, C. Free Radicals, Antioxidants in Disease and Health. *Int. J. Biomed. Sci.* **2008**, *4*, 89–96.
12. Yousaf, A.; Singh, A.; Dalal, D. Fisetin as a Neuroprotective Agent: Docking-Based Modulation of Dopaminergic and Inflammatory Pathways in Parkinson's Disease. *Neurophysiology* **2024**, *56*, 18–27, https://doi.org/10.1007/s11062-025-09981-x.
13. Zhang, Y.; Liu, Y.; Zhang, Z.; Chen, Y.; Liang, Y. Protective Effect of Astragalin on Neuroinflammation and Neurodegeneration in Alzheimer's Disease. *Int. J. Mol. Sci.* **2020**, *21*, 3250, https://doi.org/10.3390/ijms21093250.
14. Minocha, T.; Birla, H.; Obaid, A.A.; Rai, V.; Sushma, P.; Shivamallu, C.; Moustafa, M.; Al-Shehri, M.; Al-Emam, A.; Tikhonova, M.A.; Yadav, S.K.; Poeggeler, B.; Singh, D.; Singh, S.K. Flavonoids as Promising Neuroprotectants and Their Therapeutic Potential against Alzheimer's Disease. *Oxid. Med. Cell. Longev.* **2022**, *2022*, 6038996, https://doi.org/10.1155/2022/6038996.
15. Lin, J.; Zhang, W.; Wang, S.; Wang, C.; Zhang, R.; Yang, Y.; Zhou, C.; Zhang, L.; Tang, P.; Liu, J.; Jin, X.; Ma, Y. Astragalin Inhibits Neuronal Excitability and Activates Neuronal Autophagy in the ACC and LH of CFA Mice to Alleviate Inflammatory Pain and Pain-Related Emotions. *Int. Immunopharmacol.* **2025**, *148*, 114115, https://doi.org/10.1016/j.intimp.2025.114115.
16. Du, R.; Pei, H.; He, Z.; Lu, Y.; Xie, Y. Astragalin Improves Cognitive Disorder in Alzheimer's Disease: Based on Network Pharmacology and Molecular Docking Simulation. *CNS Neurosci. Ther.* **2024**, *30*, e14799, https://doi.org/10.1111/cns.14799.
17. Huang, W.J.; Zhang, X.; Chen, W.W. Role of Oxidative Stress in Alzheimer's Disease. *Biomed. Rep.* **2016**, *4*, 519–522, https://doi.org/10.3892/br.2016.630.
18. Wang, S.; Yang, Y.; Lin, J.; Zhang, W.; Yang, C.; Zhang, R.; Zhou, C.; Zhang, L.; Wang, X.; Liu, J.; Jin, X.; Ma, Y. Astragalin Activates Autophagy and Inhibits Apoptosis of Astrocytes in AD Mice via Down-Regulating the Fas/Fasl–VDAC1 Pathway. *Free Radic. Biol. Med.* **2025**, *232*, 72–85, https://doi.org/10.1016/j.freeradbiomed.2025.02.047.
19. Singh, A.; Singh, L.; Dalal, D. Mechanistic Insights into the Therapeutic Potential of Apigenin in Parkinson's Disease: An In Silico Docking and ADMET Study. *Curr. Behav. Neurosci. Rep.* **2026**, *13*, 1, https://doi.org/10.1007/s40473-026-00319-3.
20. Tao, Y.; Chen, X.; Jiang, Y.; Cai, B. A UPLC-MS/MS Approach for Simultaneous Determination of Eight Flavonoids in Rat Plasma. *Biomed. Chromatogr.* **2017**, *31*, e3828, https://doi.org/10.1002/bmc.3828.
21. He, J.; Feng, Y.; Ouyang, H.Z.; Yu, B.; Chang, Y.X.; Pan, G.X.; Zeng, S.; Li, W.; Guo, D.A. A Sensitive LC-MS/MS Method for Simultaneous Determination of Six Flavonoids in Rat Plasma. *J. Pharm. Biomed. Anal.* **2013**, *84*, 189–195, https://doi.org/10.1016/j.jpba.2013.06.019.
22. Xu, Z.L.; Xu, M.Y.; Wang, H.T.; Xu, Q.X.; Liu, M.Y.; Jia, C.P.; Zhang, H.; Zhang, W.; Zhang, Y. Pharmacokinetics of Eight Flavonoids in Rats Assayed by UPLC-MS/MS. *J. Anal. Methods Chem.* **2018**, *2018*, 4789196, https://doi.org/10.1155/2018/4789196.

23. Zheng, L.; Li, Y.; Zhou, Z.; Xiang, W.; Gong, Z.; Chen, S.; Hu, H.; Zhang, Z.; Zhang, L. Comparative Pharmacokinetics of Flavonoids in Sham-Operated and Ischemia-Reperfusion Injury Rats. *Xenobiotica* **2020**, *50*, 822–830, https://doi.org/10.1080/00498254.2019.1700319.
24. Lu, Y.; Li, N.; Zhu, X.; Pan, J.; Wang, Y.; Lan, Y.; Zhao, M.; Shi, Y.; Li, X. Comparative analysis of excretion of six major compounds of *Polygonum orientale L*. extract in urine, feces and bile under physiological and myocardial ischemia conditions in rats using UPLC–MS/MS. *Biomed. Chromatogr.* **2021**, *35*, e5174, https://doi.org/10.1002/bmc.5174.
25. Liu, J.; Zou, S.; Liu, W.; Li, J.; Wang, H.; Hao, J.; Liu, C.; Yuan, Z.; Gao, F. An Established HPLC-MS/MS Method for Evaluation of the Influence of Salt Processing on Pharmacokinetics of Six Compounds in Cuscutae Semen. *Molecules* **2019**, *24*, 2502, https://doi.org/10.3390/molecules24132502.
26. Pei, J.; Xiao, Y.; Sun, J.; Li, Z.; Zhou, H.; Liu, X.; Liu, X.; Wang, Y. Metabolic Engineering of *Escherichia coli* for Astragalin Biosynthesis. *J. Agric. Food Chem.* **2016**, *64*, 7966–7972, https://doi.org/10.1021/acs.jafc.6b03447.
27. Pei, J.; Xiao, Y.; Sun, J.; Li, Z.; Zhou, H.; Liu, X.; Wang, Y. Modulating Heterologous Pathways and Optimizing Fermentation Conditions for Biosynthesis of Kaempferol and Astragalin from Naringenin in *Escherichia coli*. *J. Ind. Microbiol. Biotechnol.* **2019**, *46*, 171–186, https://doi.org/10.1007/s10295-018-02134-6.
28. Rashed, K. Kaempferol-3-od-glucoside bioactivities: a review. *International Journal of Science Inventions Today* **2020**, *9*, 213-217.
29. Liu, Y.; Yang, X.; Gan, J.; Chen, S.; Xiao, Z.X.; Cao, Y. CB-Dock2: Improved Protein-Ligand Blind Docking by Integrating Cavity Detection, Docking and Homologous Template Fitting. *Nucleic Acids Res.* **2022**, *50*, W159–W164, https://doi.org/10.1093/nar/gkac394.
30. Shoaib, T.H.; Abdelmoniem, N.; Mukhtar, R.M.; Alqhtani, A.T.; Alalawi, A.L.; Alawaji, R.; Althubyani, M.S.; Mohamed, S.G.A.; Mohamed, G.A.; Ibrahim, S.R.M.; Hussein, H.G.A.; Alzain, A.A. Molecular Docking and Molecular Dynamics Studies Reveal the Anticancer Potential of Medicinal-Plant-Derived Lignans as MDM2-P53 Interaction Inhibitors. *Molecules* **2023**, *28*, 6665, https://doi.org/10.3390/molecules28186665.
31. Agu, P.C.; Afiukwa, C.A.; Orji, O.U.; Nwokwu, C.D.; Ejikeugwu, C.; Osuji, C.; Udu-Ibiam, O.E. Molecular Docking as a Tool for the Discovery of Molecular Targets of Nutraceuticals in Diseases Management. *Sci. Rep.* **2023**, *13*, 13398, https://doi.org/10.1038/s41598-023-40160-2.
32. Meng, X.Y.; Zhang, H.X.; Mezei, M.; Cui, M. Molecular Docking: A Powerful Approach for Structure-Based Drug Discovery. *Curr. Comput. Aided Drug Des.* **2011**, *7*, 146–157, https://doi.org/10.2174/157340911795677602.
33. Guedes, I.A.; de Magalhães, C.S.; Dardenne, L.E. Receptor-Ligand Molecular Docking. *Biophys. Rev.* **2014**, *6*, 75–87, https://doi.org/10.1007/s12551-013-0130-2.
34. Oliva, R.; Chermak, E.; Cavallo, L. Analysis and Ranking of Protein-Protein Docking Models Using Inter-Residue Contacts and Inter-Molecular Contact Maps. *Molecules* **2015**, *20*, 12045–12060, https://doi.org/10.3390/molecules200712045.
35. Prabhavathi, M.; Sahoo, B.K.; Bodapati, A.T.S.; Mishra, R.; Anand, K.; Panigrahi, P.K. An In-Vitro and In-Silico Approaches in Exploring the Molecular Contact of COVID-19 Antiviral Drug Molnupiravir with Human Serum Albumin: Effect of Binding on Protein Structure. *J. Comput. Aided Mol. Des.* **2025**, *39*, 34, https://doi.org/10.1007/s10822-025-00612-5.
36. Singh, A.; Singh, L. Acyclic Sesquiterpenes Nerolidol and Farnesol: Mechanistic Insights into Their Neuroprotective Potential. *Pharmacol. Rep.* **2024**, *77*, 31–42, https://doi.org/10.1007/s43440-024-00672-8.
37. Liu, H.; Zhong, L.; Dai, Q.; Qiu, X.; Sun, Y.; Wang, Y. Astragalin Alleviates Cognitive Deficits and Neuronal Damage in SAMP8 Mice through Upregulating Estrogen Receptor Expression. *Metab. Brain Dis.* **2022**, *37*, 3033–3046, https://doi.org/10.1007/s11011-022-01045-x.
38. Yang, C.; Zhang, R.; Wang, S.; Li, D.; Jin, Y.; Zhou, Q. Astragalin Ameliorates Cognitive Dysfunction through Inhibiting PI3K/Akt-mTOR-Mediated Autophagic Flow in Hippocampal Neurons of APP/PS1 Mice. *Res. Square* **2022**, https://doi.org/10.21203/rs.3.rs-1209539/v1.
39. Yang, C.Z.; Liu, X.Y.; Chen, L.H.; Zhao, M.J.; Li, X.H. Neuroprotective Effect of Astragalin via Activating PI3K/Akt-mTOR-Mediated Autophagy on APP/PS1 Mice. *Cell Death Discov.* **2023**, *9*, 15, https://doi.org/10.1038/s41420-023-01324-1.

40. Yao, M.; Nguyen, T.V.; Pike, C.J. Beta-Amyloid-Induced Neuronal Apoptosis Involves c-Jun N-Terminal Kinase-Dependent Downregulation of Bcl-w. *J. Neurosci.* **2005**, *25*, 1149–1158, https://doi.org/10.1523/JNEUROSCI.4736-04.2005.
41. Elmarakby, A.A.; Sullivan, J.C. Relationship between Oxidative Stress and Inflammatory Cytokines in Diabetic Nephropathy. *Cardiovasc. Ther.* **2012**, *30*, 49–59, https://doi.org/10.1111/j.1755-5922.2010.00218.x.
42. Bhaskar, K.; Miller, M.; Chludzinski, A.; Herrup, K.; Zagorski, M.; Lamb, B.T. The PI3K-Akt-mTOR Pathway Regulates Aβ Oligomer Induced Neuronal Cell Cycle Events. *Mol. Neurodegener.* **2009**, *4*, 14, https://doi.org/10.1186/1750-1326-4-14.
43. Caccamo, A.; Maldonado, M.A.; Majumder, S.; Medina, D.X.; Holtzman, D.M.; Oddo, S. Naturally Secreted Amyloid-β Increases Mammalian Target of Rapamycin (mTOR) Activity via a PRAS40-Mediated Mechanism. *J. Biol. Chem.* **2011**, *286*, 8924–8932, https://doi.org/10.1074/jbc.M110.180638.

Publisher's Note & Disclaimer